Two transcription factors, Pou4f2 and Isl1, are sufficient to specify the retinal ganglion cell fate

Fuguo Wu[a,b,c], Tadeusz J. Kaczynski[a,b,c,d], Santhosh Sethuramanujam[d,e], Renzhong Li[a,b,c], Varsha Jain[d,e], Malcolm Slaughter[c,d,e], and Xiuqian Mu[a,b,c,d,f,1]

[a]Department of Ophthalmology/Ross Eye Institute, [b]Developmental Genomics Group, New York State Center of Excellence in Bioinformatics and Life Sciences, [c]State University of New York Eye Institute, [d]Neuroscience Graduate Program, and [e]Department of Physiology and Biophysics, University at Buffalo, Buffalo, NY 14203; and [f]Cancer Center Support Grant Cancer Genetics Program, Roswell Park Cancer Institute, Buffalo, NY 14263

Edited by Jeremy Nathans, Johns Hopkins University, Baltimore, MD, and approved February 24, 2015 (received for review November 10, 2014)

As with other retinal cell types, retinal ganglion cells (RGCs) arise from multipotent retinal progenitor cells (RPCs), and their formation is regulated by a hierarchical gene-regulatory network (GRN). Within this GRN, three transcription factors—atonal homolog 7 (Atoh7), POU domain, class 4, transcription factor 2 (Pou4f2), and insulin gene enhancer protein 1 (Isl1)—occupy key node positions at two different stages of RGC development. Atoh7 is upstream and is required for RPCs to gain competence for an RGC fate, whereas Pou4f2 and Isl1 are downstream and regulate RGC differentiation. However, the genetic and molecular basis for the specification of the RGC fate, a key step in RGC development, remains unclear. Here we report that ectopic expression of Pou4f2 and Isl1 in the *Atoh7*-null retina using a binary knockin-transgenic system is sufficient for the specification of the RGC fate. The RGCs thus formed are largely normal in gene expression, survive to postnatal stages, and are physiologically functional. Our results indicate that Pou4f2 and Isl1 compose a minimally sufficient regulatory core for the RGC fate. We further conclude that during development a core group of limited transcription factors, including Pou4f2 and Isl1, function downstream of Atoh7 to determine the RGC fate and initiate RGC differentiation.

retinal development | neural development | transcription factors | cell fate specification | gene regulation

A central question in neural development is how the extreme cellular diversity in the central nervous system arises from multipotent neural progenitors. The neural retina is an excellent system to address this question because of its well-defined structure and stereotypical cellular composition. The six neuronal cell types and one glial cell type (Müller glia) form a well-laminated tissue with the various types of cells positioned at distinct layers (1). Many of these cell types are composed of multiple subtypes with distinct functions (2). All cell types in the retina originate from a common pool of retinal progenitor cells (RPCs) following a distinct temporal order (3–5). The ordered births of the retinal cell types are caused by changes of competence in RPCs for the various retinal cell types (6). Both intrinsic and extrinsic mechanisms are involved in regulating the production of the various retinal cell types, but the intrinsic factors, mostly transcription factors, appear to play more deterministic roles in directing progenitor cells toward specific cell fates (5). Many such transcription factors have been identified by loss- and gain-of-function analyses, but these studies often fail to reveal the specific roles these factors play in the development of the cell types with which they are involved (7–9). RPCs are heterogeneous, as has been demonstrated by the nonuniform expression of many RPC genes (10–13). RPCs expressing specific genes, particularly those encoding transcription factors, although still multipotent, tend to be biased for certain retinal cell types. In a few cases, specific factors dictating particular fates between binary choices have been identified. For example, Nrl switches a photoreceptor precursor from a default cone fate to a rod fate (14). The amacrine cells and horizontal cells share the same precursors, which all express Ptf1a. Expression of the onecut transcription factors (Onecut1 and Onecut2) in these precursors specifies the horizontal cell fate from the default amacrine fate (15). However, in these cases the factors involved function at relatively late stages, when the cells become very restricted in the cell fates they can adopt. How a multipotent RPC decides to adopt a particular cell fate remains an open question (5).

Retinal ganglion cells (RGCs) are the earliest-born retinal cell type, arising from a subpopulation of multipotent RPCs expressing the basic helix-loop-helix transcription factor atonal homolog 7 (Atoh7; also known as "Math5") (16, 17). Atoh7 is essential but not sufficient for the RGC fate, because, although mutations in *Atoh7* or its orthologs lead to failure of RGC formation (18–21), Atoh7-expressing RPCs give rise to all retinal cell types (16, 17). Therefore, Atoh7 does not specify the RGC fate. It is conceivable that the RGC fate is determined by factors immediately downstream of Atoh7. Two transcription factors, POU domain, class 4, transcription factor 2 (Pou4f2) and insulin gene enhancer protein 1 (Isl1), are potential candidates because of their relationships to Atoh7. Both are downstream of Atoh7 in the gene-regulatory network of RGC development and have essentially identical retinal expression patterns at the early stages of development (22–25). More importantly, they are transiently coexpressed with Atoh7 in newly formed RGCs and are the earliest known transcription factors expressed specifically in developing RGCs (10, 17). Thus, the initiation of expression of these two factors appears to coincide with RGC fate commitment. Pou4f2 and Isl1 are continuously expressed in RGCs after fate determination and are required for RGC differentiation by

Significance

Despite the progress made during the last two decades regarding the generation of retinal cell types, the mechanisms by which a retinal progenitor cell decides to adopt a particular cell type remain unclear. Using a binary knockin-transgenic system, we show that two factors, POU domain, class 4, transcription factor 2 (Pou4f2) and insulin gene enhancer protein 1 (Isl1), specify the retinal ganglion cell (RGC) fate and activate the whole gene-expression program required for ganglion cell differentiation. This study, for the first time to our knowledge, defines a set of determinant factors for any retinal cell type, offering significant insight into how cellular diversity is achieved in the central nervous system. It also provides guidance for generating RGCs in vitro for therapeutic purposes.

Author contributions: M.S. and X.M. designed research; F.W., T.J.K., S.S., R.L., V.J., and X.M. performed research; F.W., S.S., M.S., and X.M. analyzed data; and X.M. wrote the paper.

The authors declare no conflict of interest.

This article is a PNAS Direct Submission.

[1]To whom correspondence should be addressed. Email: xmu@buffalo.edu.

This article contains supporting information online at www.pnas.org/lookup/suppl/doi:10.1073/pnas.1421535112/-/DCSupplemental.

regulating two distinct but intersecting sets of downstream genes (23, 25–28). More recently, we found the Pou4f2 and Isl1 form a complex to regulate their shared target genes, further demonstrating that their functions are closely linked (29).

The emergence of RGCs from RPCs is a transition from a relatively dynamic state to a more static state. Transitions from one cellular state to another during development often are dictated by limited numbers of key regulators. Limited numbers of key regulators likely control RGC formation as well, and the expression patterns and functions of Pou4f2 and Isl1 suggest that they may be involved in RGC fate specification. In fact, ectopic expression of Pou4f2 can promote RGC genesis, although the experiments were performed in the presence of Atoh7 and the presumed RGCs thus generated were not characterized in detail (30–32). However, initial analysis of knockout mice (10) seem to argue against roles for Pou4f2 and Isl1 in RGC fate commitment, because the RGCs, although abnormal, still can form, migrate to the inner side of the retina, and project axons in the absence of Isl1 and/or Pou4f2 (23, 25, 28). Interestingly, RGCs in *Pou4f2*-knockout mice assume a hybrid identity, expressing a mixture of marker genes for RGCs, amacrine cells, and horizontal cells, suggesting that Pou4f2 indeed may play a role as an RGC specifier (33, 34). Based on these considerations, we hypothesized that the RGC fate is determined by a core group of transcription factors and that Pou4f2 and Isl1 belong to this core group. The function of this core group of transcription factors is to lock in the RGC fate irreversibly and jumpstart the RGC transcription program. These core transcription factor genes are all downstream of Atoh7 but cross-regulate each other to sustain their expression after *Atoh7* is turned off; thus the function of Atoh7 in RGC specification is to activate the expression of these core transcription factors. If this hypothesis is correct, the requirement of Atoh7 should be negated by ectopic expression of these early transcription factors in its place. To test this hypothesis, we created two mouse lines, $Atoh7^{tTA}$ and *tetO-P&I* (Pou4f2 and Isl1), and ectopically expressed Pou4f2 and Isl1 in *Atoh7*-null retinas. Our results demonstrate that, together, Pou4f2 and Isl1 are sufficient to specify the RGC fate in the developing retina.

Results

Ectopic Expression of Pou4f2 and Isl1 in Atoh7-Expressing Cells. Because Pou4f2 and Isl1 are downstream of Atoh7, and the *Atoh7*-null retina generates very few RGCs (19, 20), we reasoned that Pou4f2 and Isl1 should be able to promote RGC formation in the *Atoh7*-null retina if they determine the RGC fate. We decided to test the idea in the developing retina in vivo. For that purpose we generated two mouse alleles. The first, $Atoh7^{tTA}$, was a knockin line in which the *Atoh7* ORF was replaced by sequences encoding the tetracycline-responsive artificial transcription factor tTA (tetracycline transactivator) of the Tet-Off system (35); thus this allele was null for Atoh7 but expressed tTA under the *Atoh7* promoter (Fig. S1*A*). The other allele, *tetO-P&I*, was created by pronuclear injection. The construct used to make the transgenic mouse followed the Brainbow strategy (36), in which three cassettes encoding both Pou4f2 and Isl1 linked by sequences encoding the T2A self-cleaving peptide (37), Isl1 alone, and Pou4f2 alone were separated by loxP and lox2272 (a variant of loxP) sequences (Fig. S1*B*). The arrangement of the lox sites allows mutually exclusive recombinations by the Cre recombinase so that only one cassette would be expressed at a time, enabling the generation of three transgenic alleles from one founder line. The tetO promoter upstream of these cassettes can be activated by tTA. Our focus was on the first cassette, which expressed both Pou4f2 and Isl1.

To test if the system functioned as designed, we examined the expression of Pou4f2 and Isl1 in retinas of $Atoh7^{tTA/+}$;*tetO-P&I* embryos at embryonic day (E)14.5. At this stage, Pou4f2 and Isl1 had essentially identical expression patterns and were expressed mostly in the ganglion cell layer (GCL) and sporadically in the neuroblast layer (NBL) in the control $Atoh7^{tTA/+}$ retina (Fig. S1*C*). This expression pattern was similar to that in the wild-type retina as reported previously (25); therefore $Atoh7^{tTA/+}$ retinas were used as controls throughout this study. In the $Atoh7^{tTA/+}$; *tetO-P&I* retina, there were markedly more cells expressing both Pou4f2 and Isl1 in the NBL (Fig. S1*D*). Because *Atoh7* is active in a larger population of cells than *Pou4f2* and *Isl1* in the NBL of wild-type retinas (10), the increased number of Pou4f2- and Isl1-expressing cells indicated that tTA from the $Atoh7^{tTA}$ allele activated the *tetO-P&I* transgene and thus produced Pou4f2 and Isl1 in RPCs that normally express Atoh7. Consistent with this notion, most Pou4f2/Isl1-expressing cells in the NBL (>80%) were $Atoh7^{+}$, as indicated by colabeling of Pou4f2 and HA in the $Atoh7^{tTA/HA}$;*tetO-P&I* retina (Fig. S1 *E*–*G*) in which Atoh7 expression was marked by an HA tag (10). However, many Atoh7-expressing cells did not express Pou4f2, indicating a lapse between the expression of tTA from the *Atoh7* promoter and the activation of the *tetO-P&I* transgene.

Pou4f2 and Isl1 Specify the RGC Fate. We then examined RGC development at E14.5 in $Atoh7^{tTA/tTA}$; *tetO-P&I* embryos, which were null for *Atoh7* but should express Pou4f1 and Isl1 in Atoh7-expressing cells, using $Atoh7^{tTA/+}$ and $Atoh7^{tTA/tTA}$ as controls (Fig. 1). There were very few RGCs, as detected by anti-Pou4f2 and anti-Isl1 antibodies, in the $Atoh7^{tTA/tTA}$ retina (Fig. 1 *B*–*B*″), confirming that $Atoh7^{tTA}$ was a null allele (19, 20). There were many more cells expressing Pou4f2 and Isl1 in the NBL of the $Atoh7^{tTA/tTA}$;*tetO-P&I* retina (referred to hereafter as "$P\&I^{EE}$," for "Pou4f2 and Isl1 ectopically expressed") than in the NBL of the $Atoh7^{tTA/+}$ retina (Fig. 1 *A*–*A*″, *D*–*D*″, and *E*), indicating that $Atoh7^{tTA}$ still efficiently activated expression of the transgene in the *Atoh7*-null background. Strikingly, the GCL, as indicated by the stratum of cells positive for both Pou4f2 and Isl1 in the inner side of the retina, which was absent in the $Atoh7^{tTA/tTA}$ retina, could be readily observed in the $P\&I^{EE}$ retina, and the numbers of RGCs in the GCL were comparable to those found in the control retina (Fig. 1*E*). Thus, RGCs formed and migrated normally to the inner side of the retina when Pou4f2 and Isl1 were expressed in place of Atoh7.

To determine if RGCs could form when only one of the factors was ectopically expressed in Atoh7-expressing cells, we examined the $Atoh7^{tTA/tTA}$;*tetO-P&I;Six3-Cre* ($P\&I^{EE}$;*Cre*) retina (Fig. 1 *C*–*C*″), in which recombination by the retina-specific *Six3-Cre* would lead to the expression of only one factor in individual cells. For unknown reasons, the great majority of cells expressed only Pou4f2, but a very few expressed Isl1 or both (Fig. 1 *C*–*C*″). PCR analysis with primers for specific recombination events suggested that only recombination leading to Pou4f2, but not Isl1, expression occurred (Fig. S2). The number of cells expressing Pou4f2 in the NBL was about half the number in the $P\&I^{EE}$ retina, and the expression levels in individual cells were comparable (Fig. 1 *C*–*C*″, *D*–*D*″, and *E*). However, no GCL was formed in the $P\&I^{EE}$;*Cre* retina (Fig. 1 *C*–*C*″), suggesting that only one factor was not sufficient to specify the RGC fate.

Native Pou4f1 and Isl1 Genes Are Activated by Ectopic Pou4f2 and Isl1. At E14.5, similar to observations in the control retina (Fig. 1 *A*–*A*″), Pou4f2 and Isl1 were expressed in both the NBL and the GCL of the $P\&I^{EE}$ retina, (Fig. 1 *D*–*D*″). Because *Atoh7*, and thereby $Atoh7^{tTA}$, is active in only a subset of RPCs in the NBL but not in RGCs that already have migrated to the GCL (10, 38), we reasoned that the persistent expression of Pou4f2 and Isl1 could have resulted either from tTA and/or Pou4f2/Isl1 being very stable or from the activation of the native Pou4f2 and Isl1 genes by the ectopically expressed Pou4f2 and Isl1. If the former scenario were true, we would have expected at least some early-born

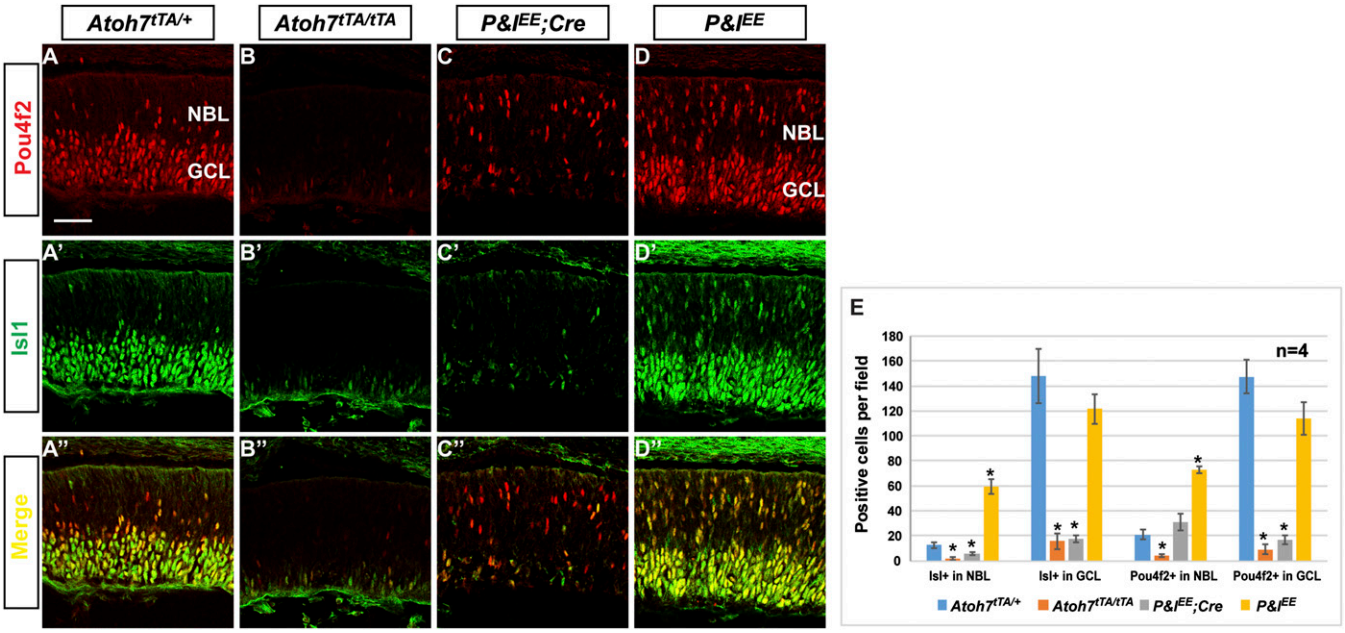

Fig. 1. Isl1 and Pou4f2 specify RGC fate. (*A–D*) Immunostaining for Pou4f2 (red) on E14.5 *Atoh7*$^{tTA/+}$ (*A*), *Atoh7*$^{tTA/tTA}$ (*B*), *P&I*^{EE}*;Cre* (*C*), and *P&I*^{EE} (*D*) retinal sections. (Scale bar, 37.5 μm.) (*A′–D′*) Immunostaining for Isl1 (green) on E14.5 retinal sections of the different genotypes. (*A″–D″*) Merged images of Pou4f2 and Isl1 staining of retinal sections with the different genotypes. Note there are more Pou4f2- and Isl1-expressing cells in the NBL of the *P&I*^{EE} retina (*D″*) than in the NBL of the *Atoh7*$^{tTA/+}$ retina (*A″*). (*E*) Counting of Pou4f2^{+} and Isl1^{+} cells in the NBL and GCL. *$P < 0.01$ (compared with *Atoh7*$^{tTA/+}$) as determined by Student's *t* test. Error bars indicate ± SD.

RGCs to lose expression by E14.5. However, the expression of Pou4f2 and Isl1 in the GCL of the *P&I*^{EE} retina was fairly uniform (Fig. 1 *D–D″*), rendering this scenario unlikely. Furthermore, at E17.5, when *Atoh7* expression had tapered down significantly (10, 38), as indicated by the decreased numbers of Pou4f2- and Isl1-expressing cells in the NBL, Pou4f2 and Isl1 remained robustly expressed in the GCL of the *P&I*^{EE} retina (Fig. 2 *D–D″*) at levels comparable to those in the *Atoh7*$^{tTA/+}$ retina (Fig. 2 *A–A″*), strongly supporting the notion that the native Pou4f2 and Isl1 genes were activated. In contrast, no appreciable expression of Pou4f2 and Isl1 expression was observed in the inner side of either the *Atoh7*$^{tTA/tTA}$ or *P&I*^{EE}*;Cre* retina (Fig. 2 *B–B″* and *C– C″*).

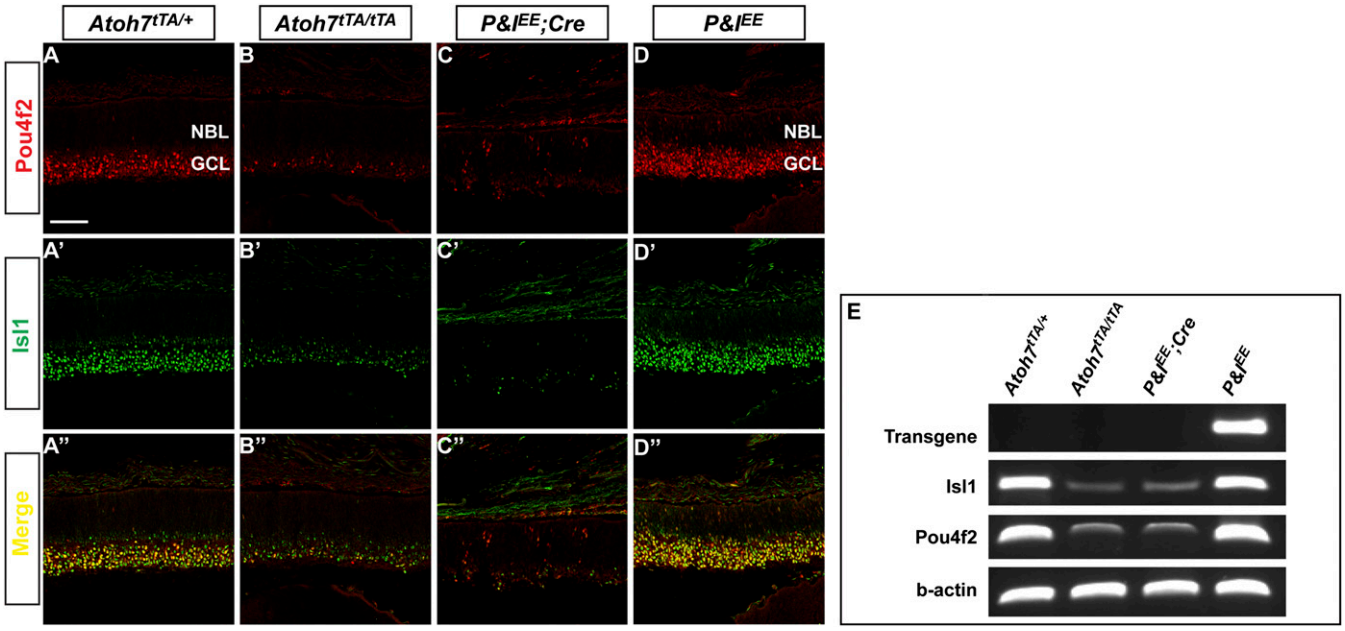

Fig. 2. Ectopic Pou4f2 and Isl1 activate the endogenous Pou4f2 and Isl1 genes. (*A–D*) Immunostaining for Pou4f2 (red) in *Atoh7*$^{tTA/+}$ (*A*), *Atoh7*$^{tTA/tTA}$ (*B*), *P&I*^{EE}*;Cre* (*C*), and *P&I*^{EE} (*D*) retinal sections at E17.5. (Scale bar, 75 μm.) (*A′–D′*) Immunostaining for Isl1 (green) of retinal sections with the different genotypes. (*A″–D″*) Merged images of Pou4f2 and Isl1 staining of retinal sections from the different genotypes. (*E*) Detection of different mRNA transcripts by RT-PCR from E17.5 retinal tissues of the different genotypes as indicated.

To validate unequivocally that the native Pou4f2 and Isl1 genes were activated in the $P\&I^{EE}$ retina, we isolated total RNA from E17.5 retinas of different genotypes and performed RT-PCR using primers that could distinguish transcripts produced by the Pou4f2-T2A-Isl1 cassette of the transgene (Fig. S1*A*) from those produced by the endogenous genes (Fig. 2*E*). As expected, transcripts from endogenous Pou4f2 and Isl1 were detected in the $Atoh7^{tTA/+}$ retina, whereas transcripts from the transgene were absent. In the $Atoh7^{tTA/tTA}$ and $P\&I^{EE}$;*Cre* retinas, very low levels of transcripts of the endogenous genes, and no transcripts from the transgene, were detected, confirming that few RGCs were produced. In the $P\&I^{EE}$ retina, however, robust levels of transcripts, not only from the transgene but also from both endogenous genes, were detected, confirming that the endogenous Pou4f2 and Isl1 genes indeed were activated by the ectopically expressed Pou4f2 and Isl1 but not by Pou4f2 alone.

Pou4f2 and Isl1 Promote Cell-Cycle Exit. Atoh7 is expressed while the retinal progenitor cells are still dividing. Although Atoh7 has been suggested to promote cell-cycle exit, it has not been unequivocally demonstrated to mark the last cell cycle (16, 39). Pou4f2 and Isl1 are expressed largely in postmitotic RGCs, although their expression can be initiated during the S phase of the last cell division (40, 41). Cells normally expressing Atoh7 in the *Atoh7*-null retina experience a transient pause in cell-cycle progression but will continue to divide (17, 39). Thus it is not clear whether Pou4f2 and Isl1 play any roles in the cell-cycle exit during RGC development. Therefore we examined the relationship between the ectopically expressed Pou4f2 and cell-cycle progression at E14.5 by BrdU pulse labeling of S-phase progenitors, which are located in the NBL (Fig. 3). In the control retina (Fig. 3 *A*–*A*′′′), consistent with previous reports, the great majority of $Pou4f2^+$ cells did not overlap with BrdU, confirming that Pou4f2, as one of the earliest RGC markers, is expressed largely postmitotically. In the *Atoh7*-null retina (Fig. 3 *B*–*B*′′′), the few $Pou4f2^+$ cells that were present were also $BrdU^-$. In the $P\&I^{EE}$ retina, the $Pou4f2^+$ cells largely did not overlap with the $BrdU^+$ cells (Fig. 3 *C*–*C*′′′), indicating that ectopic expression of Pou4f2 and Isl1 promotes cell-cycle exit. Our finding suggests that cell-cycle exit and RGC fate commitment are coupled and that Pou4f2 and Isl1 are involved in both processes.

RGCs Generated by Ectopic Pou4f2 and Isl1 Have a Largely Normal Gene-Expression Program. An important question was how normal were the RGCs generated by ectopic Pou4f2 and Isl1. This question was addressed first by analyzing how completely the gene expression program for RGC differentiation was activated in the $P\&I^{EE}$ retina. To that end, we analyzed 11 RGC-expressed genes through immunostaining or in situ hybridization (Fig. 4). These genes are expressed in the RGCs of the control retina, but their expression is severely diminished in the *Atoh7*-null retina (Fig. 4) (15, 22–24, 42, 43). Among them, *Nflm*, *Pgp9.5*, *Pou4f1*, *Sncg*, and *Rbpms* are dependent on Pou4f2 and/or Isl1 for expression, whereas *Oc1*, *Stmn2*, *Sox4*, *Sox11*, *Ina*, and *Eya2* are not. Nevertheless, all these genes except *Eya2* were expressed robustly in the $P\&I^{EE}$ retina (Fig. 4), indicating that the cells in the presumed GCL were bona fide RGCs. The finding that genes normally independent of Pou4f2 or Isl1 also were activated indicated nearly complete activation of the RGC differentiation program in the $P\&I^{EE}$ retina.

We also examined the expression of *Ccnd1* (*cyclin D1*) and *Gli1*, two genes expressed in RPCs (Fig. 4). These two genes are regulated by sonic hedgehog secreted from the RGCs through a feedback loop (44, 45). The expression of these two genes is compromised significantly in *Atoh7*-, *Isl1*-, and *Pou4f2*-null retinas (Fig. 4) (22–24). In the $P\&I^{EE}$ retina, the expression of both *Ccnd1* and *Gli1* reached levels comparable to those in the heterozygous control (Fig. 4). These results imply that the non–cell-autonomous gene-regulation pathway mediated by RGC-secreted molecules also resumed in the $P\&I^{EE}$ retina.

RGCs Generated by Pou4f2 and Isl1 Survive to Adulthood. In both *Isl1*- and *Pou4f2*-null retinas RGCs are born initially but do not

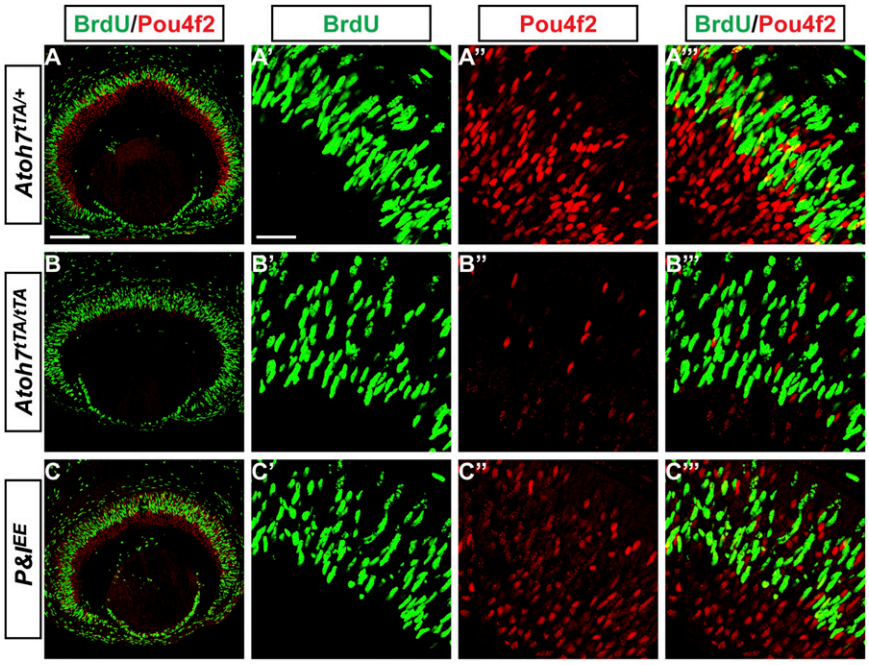

Fig. 3. Isl1 and Pou4f2 promotes cell-cycle exit. (*A*) Immunostaining of BrdU (green) and Pou4f2 (red) on $Atoh7^{tTA/+}$ retinal sections at E14.5. (Scale bar, 150 μm.) (*A*′–*A*′′′) High-magnification images of *A* in separate (red for Pou4f2 and green for BrdU) and merged channels. (Scale bar, 25 μm.) (*B*) Costaining of BrdU and Pou4f2 on E14.5 $Atoh7^{tTA/tTA}$ retinal sections. (*B*′–*B*′′′) High-magnification images of *B* in separate and merged channels. (*C*) Costaining of BrdU and Pou4f2 on E14.5 $P\&I^{EE}$ retinal sections. (*C*′–*C*′′′) High-magnification images of *C* in separate and merged channels.

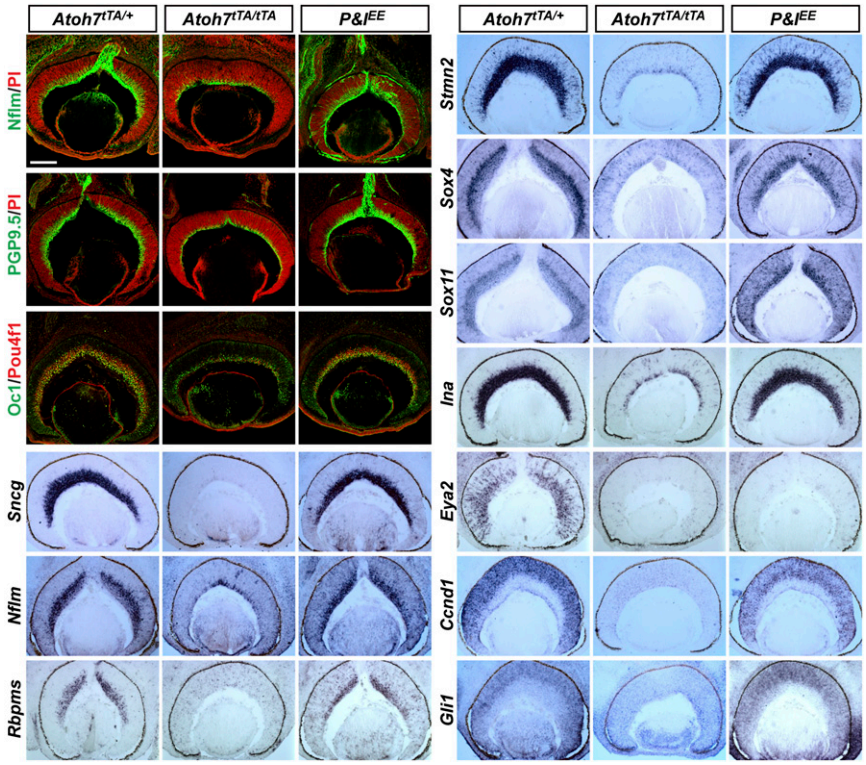

Fig. 4. The gene-expression program in the RGCs of the *P&I*^{EE} retina is almost fully activated. Immunostaining for Nflm (green), PGP9.5 (green), Onecut1 (green), and Pou4f1 (red) and in situ hybridization for *Sncg*, *Nflm*, *Rbpms*, *Stmn2*, *Sox4*, *Sox11*, *Ina*, *Eya2*, *Cyclin D1* (*Ccnd1*), and *Gli1* in *Atoh7*$^{tTA/+}$, *Atoh7*$^{tTA/tTA}$, and *P&I*^{EE} retinal sections at E14.5. With the exception of *Eya2*, these genes are fully activated in the *P&I*^{EE} retina. (Scale bar, 150 μm.)

differentiate normally, and the majority die through apoptosis by birth (P0) (23, 25, 27, 28). Therefore, it was important to know if the RGCs generated in the *P&I*^{EE} retina could survive to postnatal stages. At postnatal day (P)18, we observed that the *P&I*^{EE} retina possessed an optic nerve that was similar in thickness to that of the control retina (Fig. 5*A*), indicating that the RGCs

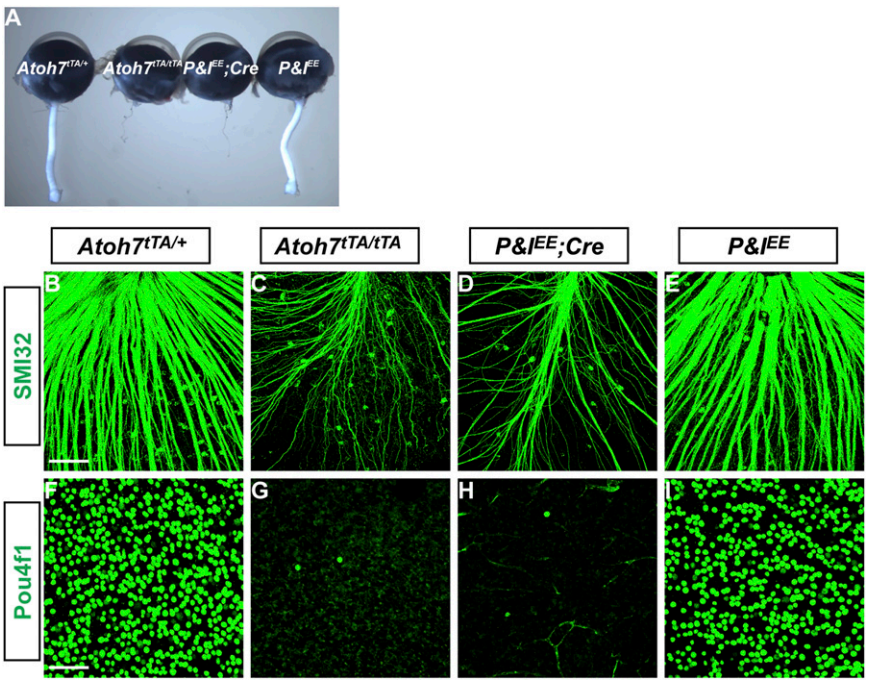

Fig. 5. RGCs in the *P&I*^{EE} retina survive to postnatal stages. (*A*) The optic nerves from P18 *Atoh7*$^{tTA/+}$, *Atoh7*$^{tTA/tTA}$, *P&I*^{EE}*;Cre*, and *P&I*^{EE} retinas. (*B–E*) Whole-mount immunostaining of RGC axons with SMI32 in *Atoh7*$^{tTA/+}$, *Atoh7*$^{tTA/tTA}$, *P&I*^{EE}*;Cre*, and *P&I*^{EE} retinas at P18. (Scale bar, 150 μm.) (*F–I*) Immunolabeling of RGCs with anti-Pou4f1 in whole-mount retinas of the various genotypes at P18. (Scale bar, 75 μm.)

survived to postnatal stages. However, the *Atoh7*$^{tTA/tTA}$ retina displayed only a rudimentary optic nerve, as previously reported (20) (Fig. 5*A*). The *P&I*^{EE}*;Cre* retina was similar to the *Atoh7-null* retina and also possessed only a very thin optic nerve (Fig. 5*A*). Consistently, by whole-mount staining for neurofilament heavy chain with SMI32, we observed well-fasciculated optic fibers in the *P&I*^{EE} retina at P18 which were similar in number to those in the control retina and projected normally to the optic disk (Fig. 5 *B* and *E*). In contrast, very few optic fibers could be seen in the *Atoh7*$^{tTA/tTA}$ and *P&I*^{EE}*;Cre* retinas (Fig. 5 *C* and *D*). Additionally, staining for Pou4f1 further confirmed that there were equivalent numbers of RGCs in the P18 *P&I*^{EE} retina and the control (Fig. 5 *F* and *I*), in contrast with the *Atoh7*$^{tTA/tTA}$ and *P&I*^{EE}*;Cre* retinas, which displayed very few RGCs (Fig. 5 *G* and *H*). These observations demonstrated that the RGCs generated by ectopically expressed Pou4f2 and Isl1 were maintained in the mature retina.

Development of RGC Subtypes in the *P&I*^{EE} Retina. There are about 20 RGC subtypes based on function and morphology (2, 46). These subtypes are involved in detecting the various features of vison. Molecular markers are available for only a few of the subtypes (46). Nevertheless, we used some of these markers to examine whether the corresponding RGC subtypes were present in the *P&I*^{EE} retina. Tbr2 (also known as "Eomes") is expressed in a subset of RGCs, from which the intrinsically photosensitive RGCs (ipRGCs) arise (47–49). At E14.5, by coimmunostaining for Tbr2 and Pou4f2, we observed that Tbr2 was expressed in equivalent numbers of RGCs in the *P&I*^{EE} retina and the control retina, although its expression was almost completely absent in the *Atoh7*$^{tTA/tTA}$ retina (Fig. 6 *A*–*C* and *M*). Consistent with these results, there were essentially no ipRGCs, as determined by anti-melanopsin immunostaining, in the *Atoh7*$^{tTA/tTA}$ retina at P30. However, there were a substantial number of ipRGCs in the *P&I*^{EE} retina (Fig. 6 *D*–*F* and *M*). CART (cocaine and amphetamine-regulated transcript) is a marker for ON–OFF direction-selective RGCs (Fig. 6 *G* and *M*) (50), which could barely be detected in the *Atoh7*$^{tTA/tTA}$ retina (Fig. 6 *H* and *M*); in contrast, numerous CART^{+} RGCs were observed in the *P&I*^{EE} retina (Fig. 6 *I* and *M*). Calbindin is expressed in both displaced amacrine cells and a subset of RGCs in the GCL (51). Calbindin^{+} RGCs could be distinguished from displaced amacrine cells by colabeling with Pou4f1. It is apparent that the calbindin^{+} RGCs are a subclass of RGCs (Fig. 6*J*), although their physiological function is not known, because only a subset of Pou4f1^{+} cells expressed calbindin. In the *Atoh7*$^{tTA/tTA}$ retina, the great majority of calbindin^{+} cells were Pou4f1^{-} (Fig. 6*K*), indicating that they were displaced amacrine cells. In the *P&I*^{EE} retina, however, the numbers of calbindin^{+}Pou4f1^{+} cells were comparable to those found in the control retina (Fig. 6 *L* and *M*). These results indicate both that the generic RGCs were formed and maintained in the *P&I*^{EE} retina and that their specification into individual subtypes occurred normally.

Development of Other Retinal Cell Types in the *P&I*^{EE} Retina. We also examined the development of other retinal cell types, including amacrine cells, bipolar cells, Müller glial cells, cones, rods, and horizontal cells in the *P&I*^{EE} retina with various cell-type–specific markers at P18. Most of these retinal cell types appeared normal both in number and position (Fig. S3). Notably, cone photoreceptors, which are overproduced in the *Atoh7*-null retina (Fig. S3 *K* and *S*) (20), were normal in the *P&I*^{EE} retina (Fig. S3 *L* and *S*). The *Atoh7*-null retina often displays disrupted lamination in areas within the retina (Fig. S3 *K* and *N*) (20). Interestingly, this defect also was corrected in the *P&I*^{EE} retina (Fig. S3 *L* and *O*), although currently we do not understand the underlying mechanisms. Horizontal cells also have been reported to be underproduced in *Atoh7*-null retinas (Fig. S3 *Q* and *S*) (16). We observed a further reduction of horizontal cells by flat-mount staining with anti-calbindin in the *P&I*^{EE} retina (Fig. S3 *R* and *S*). It is possible that some of the progenitor cells normally becoming horizontal cells adopted the RGC fate, leading to fewer horizontal cells being formed.

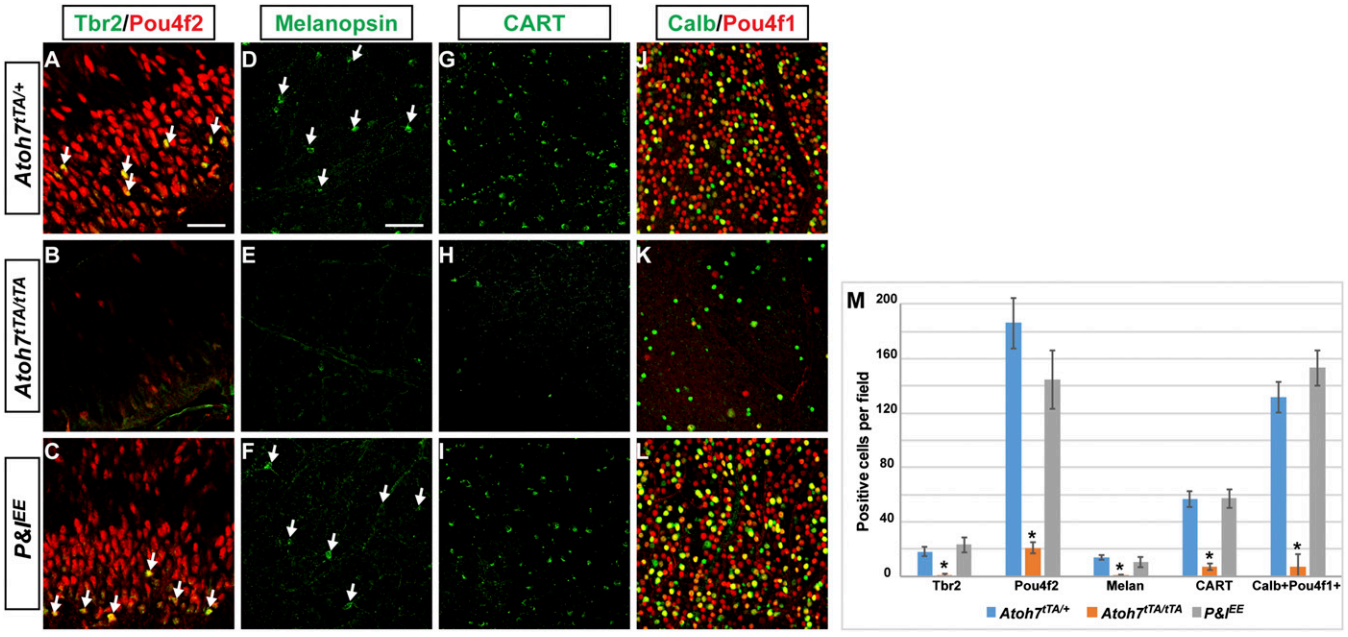

Fig. 6. RGC subtypes form in the *P&I*^{EE} retina. (*A*–*C*) Immunostaining for Tbr2 (green) and Pou4f2 (red) in E14.5 *Atoh7*$^{tTA/+}$ (*A*), *Atoh7*$^{tTA/tTA}$ (*B*), and *P&I*^{EE} (*C*) retinal sections. Arrows indicate the Tbr2^{+} cells. (Scale bar, 25 μm.) (*D*–*F*) Flat-mount immunostaining for melanopsin to visualize ipRGCs (indicated by arrows) in retinas of different genotypes at P30. (Scale bar, 75 μm.) (*G*–*I*) Staining for CART to visualize dsRGCs in retinas of different genotypes at P30. (*J*–*L*) Costaining of Calbindin (Calb, green) and Pou4f1 (red) in flat-mount retinas of the different genotypes at P30. (*M*) Cell counting of the different RGC subtypes in retinas with the different genotypes. Melan, melanopsin. *$P < 0.01$ (compared with *Atoh7*$^{tTA/+}$) as determined by Student's *t* test. Error bars indicate ± SD.

RGCs in the *P&I*^{EE} Retina Show Robust Light-Evoked Spike Activity. Ultimately, we wanted to know if the RGCs in the *P&I*^{EE} retina were normal in their physiological function. To that end, we investigated whether the ganglion layer cells (GLCs) of *P&I*^{EE} mice had light-evoked spike activity. Spike activity was measured either simultaneously from a population of cells using the multiple electrode array (MEA) (Fig. 7*F*) or from single cells using patch-clamp recording. In total, we were able to observe light-evoked spike activity in five of five retinas tested from three P30 animals. We tested the ability of GLCs in the *P&I*^{EE} retina to extract the ON/OFF and transient/sustained information from the light stimulus. ON cells respond with increased spike activity after light onset, and OFF cells respond with increased light activity after light offset. Transient cells respond with a short burst of spikes immediately after the onset or offset of light stimulus, but sustained cells respond with sustained spike activity for the duration of the stimulus. The responses of GLCs to a square pulse of light can be broadly classified as ON-sustained, OFF-sustained, ON-transient, OFF-transient, and ON-OFF transient (52). As shown in Fig. 7, each of these response types was found in multiple GLCs of the *P&I*^{EE} retina (Fig. 7 *A*–*E*).

The light responses were robust and precise across several light trials as shown in the raster plot of a single transient ON cell spike activity (Fig. 7*G*) and in the superimposed light-evoked synaptic currents (Fig. 7 *H* and *I*), indicative of stable synapses. We isolated the light-evoked excitatory postsynaptic currents (EPSCs) or inhibitory postsynaptic currents (IPSCs) by voltage clamping the recorded cell at −60 mV or 0 mV, respectively (Fig. 7 *H*–*J*) (53). In response to light, both EPSCs and IPSCs were robust and precise across at least five light trials (superimposed traces), confirming the stability of bipolar-RGC and amacrine-RGC synapses (54, 55). We also observed miniature spontaneous EPSCs and IPSCs in the dark, again indicating that these cells form synapses with both bipolar and amacrine cell inputs (Fig. 7 *H*, *Inset* and *I*, *Inset*) (56). Both light-evoked EPSCs and IPSCs were of amplitudes commonly observed in the normal mouse retina (Fig. 7*J*) (52).

Although the GLCs we tested may have included some displaced amacrine cells, the presence of multiple cells with all types of responses seen in wild-type retinas suggested that all major physiological RGC subtypes were present in the *P&I*^{EE} retina and were functionally incorporated into the visual circuitry. This result further supports the conclusion that Pou4f2 and Isl1 are sufficient to specify the RGC fate and activate the RGC differentiation program.

Discussion

In this study, we show that in the absence of Atoh7, ectopic expression of Pou4f2 and Isl1 leads to essentially normal development of RGCs, which survive to postnatal stages, diversify into distinct subtypes, and functionally integrate into the visual circuitry. Because the Atoh7-expressing cells in the *Atoh7*-null retina adopt all retinal cell types but RGCs, and Pou4f2 and Isl1 are the earliest factors expressed in the RGC lineage, our results unequivocally demonstrate that Pou4f2 and Isl1 determine the RGC fate. Further, we show that ectopic Pou4f2 and Isl1 can activate the native Pou4f2 and Isl1 genes. These observations lead us to a model of RGC determination in development (Fig. 8). In this model, the function of Atoh7 is to activate the core RGC fate-determining transcription factor genes including *Pou4f2* and *Isl1* in a subset of Atoh7-expressing RPCs. Once this core group of genes is activated, the transcription factors sustain their own expression by cross-regulation and/or autoregulation and no longer rely on the upstream activator Atoh7. This core group of transcription factors then activates the gene-expression program required for RGC differentiation. In the *P&I*^{EE} retina, although Atoh7 is not present, ectopic Pou4f2 and Isl1 activate the endogenous genes encoding this core group of factors, thereby leading to almost normal RGC development. This model also explains why RGCs, although abnormal, still form in the *Pou4f2*- and *Isl1*-null retinas, because other members in the core group still can activate a substantial, although incomplete, part of the RGC developmental program.

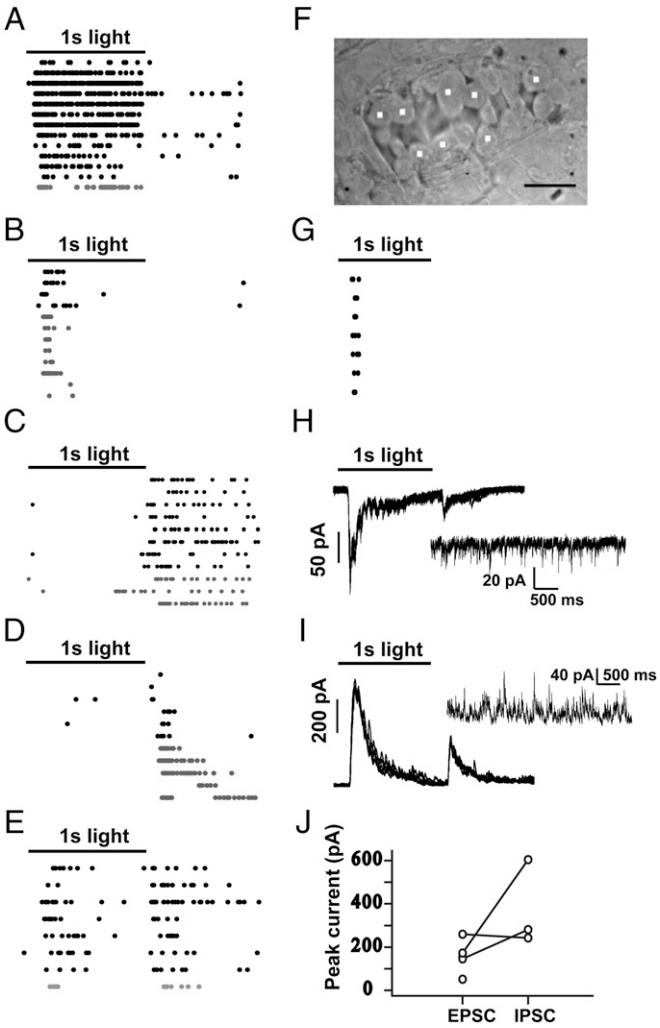

Fig. 7. RGCs in the *P&I*^{EE} retina are physiologically functional and show robust light-evoked spike activity. (*A*–*E*) Spike raster plots for cells recorded using both MEA and single-cell patch clamping. (*A*) ON-sustained cells showed sustained spike activity for the onset of light but stopped spiking at light offset. Each row shows the response of a single cell (n = 13). The light stimulus (1 s in duration) is represented by the black bar on top. The black traces show cells recorded in an MEA; the gray traces show cells recorded by single-cell patch-clamp recording. (*B*) ON-transient cells showed brief spike activity at light onset (n = 12). (*C*) OFF-sustained cells exhibited sustained activity at light offset (n = 11). (*D*) OFF-transient cells had phasic spike activity at light offset (n = 11). (*E*) ON-OFF cells showed spike activity at both light onset and offset (n = 8). (*F*) A window created in the GCL to record light-evoked activity in single cells. Even in this small window, a majority of cells (white marks) responded with spike activity to light. (Scale bar, 25 μm.) (*G*) Light-evoked spike activity of an ON transient cell in seven trials. The light response was robust and precise across trials. (*H*) Light-evoked EPSCs of the cell shown in *G* for five trials. Cells were held at Vh = −60 mV to isolate EPSCs. The responses of the trials are shown superimposed, illustrating the precision of the responses. (*Inset*) Sample spontaneous EPSCs evoked in the absence of light. (*I*) Light-evoked IPSCs of a cell shown in *G* for five trials (Vh = 0 mV). (*Inset*) Spontaneous IPSCs observed in the absence of light. (*J*) Comparison of peak light-evoked EPSCs in five cells and light-evoked IPSCs in three cells. Each line indicates the EPSC and IPSC recorded from the same cell.

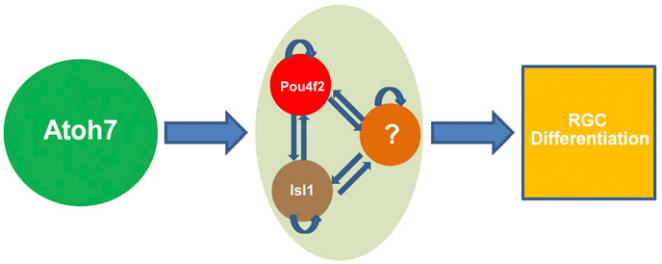

Fig. 8. A model for RGC fate determination in development. In this model, Atoh7 activates a small set of transcription factor genes, including *Pou4f2* and *Isl1*, in a subset of Atoh7-expressing cells. Expression of this group of transcription factors determines the RGC fate. The question mark indicates the unidentified member(s) of this group. Once expressed, these factors can sustain their own expression, and Atoh7 becomes disposable. Arrows designating regulations between factors within the core group (including Pou4f2 and Isl1) are conceptual and do not necessarily implicate direct regulation (see text). This core group of transcription factors in turn activates the whole gene-expression program for RGC differentiation.

Additional factors must be involved (Fig. 8), because there are RGC genes whose expression does not change in *Isl1*-, *Pou4f2*-, or *Isl1*/*Pou4f2* double-null retinas (22, 23, 29). Nevertheless, most of these genes are activated by ectopically expressed Pou4f2 and Isl1 in the *Atoh7*-null background. This observation actually is consistent with our model, in which the transcription factors in the core group cross-regulate each other's expression. Therefore, although only Pou4f2 and Isl1 are ectopically expressed initially, the unknown member(s) of this core group also can be activated, leading to an almost complete activation of RGC differentiation program. Currently the details of the cross-regulation, either direct or indirect, and the autoregulation of these factors are not very clear, but it is known that Isl1 is required for the sustained expression of Pou4f2 (23). It also is not clear how many transcription factors belong to this core group, but it is likely that there are not very many, considering the numbers of genes whose expression is affected in the *Pou4f2*-, *Isl1*-, and *Atoh7*-null retinas (23).

Candidates for the unknown factors include Sox4 and Sox11, because they are downstream of Atoh7 but are independent of Pou4f2 and Isl1, and double knockout of *Sox4* and *Sox11* leads to severely compromised RGC production (43). Our observations that *Sox4* and *Sox11* are activated by ectopic Pou4f2 and Isl1 also support this idea, although further experimental confirmation is needed. The finding that *Eya2* expression is not rescued by ectopic Isl1 and Pou4f2 is intriguing. *Eya2* is highly expressed in developing RGCs with a pattern very similar, if not identical, to those of Pou4f2 and Isl1 and thus is an early RGC transcription factor (42, 57). Its expression is dependent on Atoh7 but is independent of Pou4f2 and Isl1 (42). The fairly normal development of RGCs in the $P\&I^{EE}$ retina in the absence of Eya2 expression suggests that Eya2 may play only a minor role in RGC development. However, given its specific expression patterns during retinal development, it is highly possible that Eya2 may have a specific role, independent of Pou4f2 and Isl1, in RGC development.

RGC fate determination, exit of cell cycle, and migration to the future GCL are three concomitant aspects of RGC genesis. Ectopic expression of Pou4f2 and Isl1 led not only to RGC formation but also to their cell-cycle exit and correct migration, indicating that Pou4f2 and Isl1 regulate all three aspects and that the three aspects are tightly linked. Cell-cycle exit and cell migration during RGC development thus must be carried out by genes downstream of Pou4f2 and Isl1. How cell-cycle exit and directional cell migration are regulated and coordinated with cell-fate specification remains poorly understood but will be addressed only by identifying the genes involved in these processes.

Another remaining question is the mechanism by which Atoh7 activates *Pou4f2* and *Isl1*. Because Atoh7 does not activate *Pou4f2* and *Isl1* in all cells, a stochastic mechanism may be at play. This stochastic mechanism could result from the natural fluctuation of Atoh7 levels among the Atoh7-expressing cell population, because the levels of Atoh7 affect the numbers of RGCs produced (58). It also is possible that Atoh7 collaborates with another factor, which is not available in all Atoh7-expressing progenitors, to activate *Pou4f2* and *Isl1*. A related question is whether the final cell division of Atoh7-expressing cells before RGC fate commitment is symmetrical or asymmetrical, i.e., whether *Pou4f2* and *Isl1* are activated in both daughter cells from the last cell division to specify them into the RGC fate. This issue may be resolved by clonal labeling experiments in the future.

Because RPCs are heterogeneous, and their competence for retinal cell types changes over time, it would be interesting to know whether Pou4f2 and Isl1 could direct RGC formation in different cellular contexts, e.g., in non–Atoh7-expressing RPCs from either temporally appropriate (early) or inappropriate (late) developmental stages. In this study, we ectopically expressed Pou4f2 and Isl1 in Atoh7-expressing cells in the absence of Atoh7. Because the *Atoh7*-null RPCs normally expressing Atoh7 give rise to all retinal cell types but RGCs, it is not clear whether they still possess unique properties or are more similar to other RPCs that do not express Atoh7 at the early stage. This issue could be addressed in the future by analyzing the transcriptomes of the different RPC populations in the presence and absence of Atoh7 and by ectopically expressing Pou4f2 and Isl1 in non–Atoh7-expressing cells at different stages.

RGC death is involved in several retinal diseases such as glaucoma and optic ischemia, which often lead to vision loss and even blindness (59, 60). Much effort has been undertaken to produce RGCs for cell-based therapies directly in vitro from various stem cells (61–63). Unlike other retinal cell types such as photoreceptors, these efforts suffer a major obstacle: the low efficiencies for the RGC lineage. Our finding that Pou4f2 and Isl1 together can determine the RGC fate and promote their genesis will provide guidance for those efforts.

Materials and Methods

Generation of Mouse Lines. The $Atoh7^{tTA}$ allele was generated as shown in Fig. S1*A*. Using recombineering (23), a targeting construct was generated by replacing the *Atoh7* ORF with the tTA ORF followed by a PGK-Neo cassette. The construct was used to electroporate the G4 129xC57BL/6 F1 hybrid ES cells (23, 64). Two positive clones, identified by Southern blot hybridization, were injected into C57/BL6 blastocysts to generate chimeric mice, which then were mated with wild-type C57BL/6 females for germline transmission. Please note that this line was different from another *Atoh7-tTA* line, which was mistargeted with *Atoh7* still being expressed and functional (42). The *tetO-P&I* mice were made by pronuclear injection. A transgenic construct containing the Pou4f2- and Isl1-expressing cassettes under the tetO promoter, as shown in Fig. S1*B*, was made by PCR and standard cloning. Positive founder pups (two were obtained) were identified by PCR for the presence of the transgene. Only one line was responsive to tTA from $Atoh7^{tTA}$ and was used in this study. All mice were maintained in a C57/BL6 × 129 genetic background. All procedures using mice conform to the US Public Health Service Policy on Humane Care and Use of Laboratory Animals (65) and were approved by the Institutional Animal Care and Use Committees of Roswell Park Cancer Institute and the University at Buffalo.

Immunofluorescence Staining. Immunofluorescence staining followed a protocol we have described previously (15, 66, 67). Briefly, after fixation with 4% paraformaldehyde for 30 min and three washings with PBS (pH7.4) plus 0.1% Tween 20 (PBST), embryos (E14.5) or eyes (P0 and older) were embedded in Optimum Cutting Temperature (OCT) compound. The embedded tissues then were sectioned at 16 μm. For immunofluorescence labeling, the sections were washed three times for 10 min with PBST and blocked with

2% (wt/vol) BSA in PBST for 1 h and then were incubated with primary antibodies for 1 h. After three 10-min washings with PBST, fluorescent dye-conjugated secondary antibodies (Life Technologies) were applied to the sections, incubated for 1 h, and washed with PBST. When necessary, the sections were counterstained with propidium iodide. For whole-mount staining, the same general procedure was followed, except that the incubation time and washing time were considerably longer. Sources of all antibodies and their dilutions also have been published previously (15, 66, 67). Counting of positive cells was performed as described previously (66), and the significance of difference ($P < 0.1$) between various genotypes and the control was determined by Student's *t* test.

Images were acquired with a Leica TCS SP2 confocal microscope. In some cases, the contrast of images was adjusted in Adobe Photoshop. The adjustments were made to the same degree for sections of different genotypes for the same experiment.

In Situ Hybridization. In situ hybridization followed a protocol described previously (15, 66). The tissues were fixed in 4% (wt/vol) paraformaldehyde overnight, embedded in OCT, and sectioned at 16 μm. Digoxigenin (Dig)-labeled anti-sense probes were made by in vitro transcription (22). The sections then were hybridized with the probes at 65 °C overnight in hybridization solution [1× salt, 50% (vol/vol) formamide, 10% (wt/vol) dextran sulfate, 1mg/mL tRNA, 1× Denhardt's solution (Life Technologies)] followed by three 30-min washings with washing buffer (1× SSC, 50% formamide, 0.1% Tween 20) at 60 °C. The slides then were incubated twice with 1× MABT buffer (0.1 M maleic acid, 0.25 M NaCl, 0.1% Tween 20, pH7.5) at room temperature, blocked with 20% (vol/vol) sheep serum/2% (wt/vol) Blocking Reagent (Roche), and incubated overnight with alkaline phosphatase-conjugated anti-Dig (1:1,500; Roche) at room temperature. Then they were washed thoroughly with 1× MABT and were developed with nitroblue tetrazolium/5-bromo-4-chloro-3-indolyl-phosphate to the desired signal intensities.

RT-PCR. Total RNA isolation from retinal tissues and reverse transcription reaction were carried out as described previously (66). cDNA equivalent to 40 ng of total RNA then was used as template for each PCR. The primers used to detect the different transcripts were *tetO-P&I*, forward 5′-CGA AAA GCT GGA TCT CAA GA-3′, reverse 5′-AAT ACT GAT TAC ACT CCG CA-3′; *Isl1*, forward 5′-TTG CAA AGC GAC ATA GAT CA-3′, reverse 5′-CAT TGA CTG GGT CGT TAA AT-3′; *Pou4f2*, forward 5′-TCT GGA AGC CTA CTT CGC CA-3′, reverse 5′-CTG GGT TCA CAT TTA CCG GA-3′; β-actin, forward 5′-ATC ATG TTT GAG ACC TTC AAC A-3′, reverse 5′-GGT CAG GAT CTT CAT GAG GTA-3′. The PCR products were resolved on a 1.5% (wt/vol) agarose gel.

GLC Recording. To prepare tissue for electrophysiology, animals were killed by overdose of 1–3% (vol/vol) halothane and were decapitated, and the eyes were enucleated. The retinal whole-mount preparation has been described in detail elsewhere (53). The tissue was constantly superfused with oxygenated Ringer's solution containing 111 mM NaCl, 2.5 mM KCl, 1 mM CaCl2, 1.6 mM MgCl2, 22 mM NaHCO3, and 10 mM dextrose buffered to pH 7.4 using bubble 95% (vol/vol) O2 and 5% (vol/vol) CO_2. A gravity-fed perfusion system was used to maintain a flow rate of ∼1.5 mL/min.

For MEA recordings the flat mounted retina was inverted onto an MEA with 60 electrodes of 10-um diameter spaced 100 um apart (Multi Channel System; MCS GmbH). The light responses were recorded 60 min after the retina was placed in the MEA chamber. The data were acquired and analyzed using the Multi Channel System software. The signals were filtered between 20 Hz (low cutoff) and 700 Hz (high cutoff). The spikes were sorted by setting a threshold higher than 30 μV. A diffuse full-field light stimulus from a white light-emitting diode was presented for 1 s with an interstimulus time interval of 10 s. At least 20 trials were recorded for each experiment. The irradiance calculated between 300 and 800 nm of the LED was ∼1 $\mu W \cdot cm^{-2} \cdot s^{-1}$, measured by an RPS900-R wideband spectroradiometer (International Light).

The single-cell patch-clamp recording experiments were performed under infrared light as described in detail elsewhere (53). In brief, recordings were made from GLCs at room temperature. Extracellular spike activity was measured with a loose seal (25–50 MΩ) using an 8–10 MΩ electrode filled with Ringer's solution. Neurons were patched for whole-cell recordings using a separate 5–7 MΩ electrode containing either (*i*) potassium internal (115 mM potassium gluconate, 5 mM KCl, 1 mM MgCl2, 10 mM Hepes, and 10 mM EGTA buffered to pH 7.4 with KOH) or (*ii*) cesium internal (112.5 mM CsMeSO3, 9.7 mM KCl, 1 mM MgCl2, 10 mM Hepes, 10 mM EGTA, and QX-314.Cl buffered to pH 7.4 with CsOH).

Data were acquired using a Multiclamp 700B Amplifier (Molecular Devices). Analog signals were low-pass–filtered at 2 kHz and sampled at 10 kHz with the Digidata 1322A analog-to-digital board (Molecular Devices). Clampex 10.1 software (Molecular Devices) was used to control the voltage command outputs, acquire data, and trigger stimuli. Photoreceptors were stimulated by a 200-μm spot from a green light-emitting diode (LED, λmax = 520 nm) projected through the objective lens. The irradiance calculated between 500 and 540 nm of the LED was ∼1.6 $\mu W \cdot cm^{-2} \cdot s^{-1}$, measured by an RPS900-R wideband spectroradiometer (International Light). A 1-s light stimulus was presented every 15 s.

The peak light-evoked EPSCs and IPSCs were monitored only when the EPSP induced spike activity. For example, the cell in Fig. 7*H* had excitatory currents at both light onset and offset, but spike activity was induced only after light onset (Fig. 7*G*). Hence only the light onset EPSC and IPSC peaks were used to represent this cell in Fig. 7*J*.

ACKNOWLEDGMENTS. We thank other members of the X.M. laboratory and members of Department of Ophthalmology and the Developmental Genomics Group, University of Buffalo, for helpful discussions. The *Atoh7*^{tTA} and *tetO-P&I* alleles were created with the help of the Gene Targeting and Transgenic Resource Core at the Roswell Park Cancer Institute. This project was supported by National Eye Institute Grants EY020545 (to X.M.) and EY05725 (to M.S.), by the Whitehall Foundation (X.M.), and by an unrestricted grant from Research to Prevent Blindness (to X.M.).

1. Wässle H, Boycott BB (1991) Functional architecture of the mammalian retina. *Physiol Rev* 71(2):447–480.
2. Masland RH (2012) The neuronal organization of the retina. *Neuron* 76(2):266–280.
3. Cepko CL, Austin CP, Yang X, Alexiades M, Ezzeddine D (1996) Cell fate determination in the vertebrate retina. *Proc Natl Acad Sci USA* 93(2):589–595.
4. Young RW (1985) Cell differentiation in the retina of the mouse. *Anat Rec* 212(2): 199–205.
5. Cepko C (2014) Intrinsically different retinal progenitor cells produce specific types of progeny. *Nat Rev Neurosci* 15(9):615–627.
6. Livesey FJ, Cepko CL (2001) Vertebrate neural cell-fate determination: Lessons from the retina. *Nat Rev Neurosci* 2(2):109–118.
7. Xiang M (2013) Intrinsic control of mammalian retinogenesis. *Cell Mol Life Sci* 70(14): 2519–2532.
8. Bassett EA, Wallace VA (2012) Cell fate determination in the vertebrate retina. *Trends Neurosci* 35(9):565–573.
9. Swaroop A, Kim D, Forrest D (2010) Transcriptional regulation of photoreceptor development and homeostasis in the mammalian retina. *Nat Rev Neurosci* 11(8):563–576.
10. Fu X, et al. (2009) Epitope-tagging Math5 and Pou4f2: New tools to study retinal ganglion cell development in the mouse. *Dev Dyn* 238(9):2309–2317.
11. Brzezinski JA, IV, Kim EJ, Johnson JE, Reh TA (2011) Ascl1 expression defines a subpopulation of lineage-restricted progenitors in the mammalian retina. *Development* 138(16):3519–3531.
12. Hafler BP, et al. (2012) Transcription factor Olig2 defines subpopulations of retinal progenitor cells biased toward specific cell fates. *Proc Natl Acad Sci USA* 109(20): 7882–7887.
13. Trimarchi JM, Stadler MB, Cepko CL (2008) Individual retinal progenitor cells display extensive heterogeneity of gene expression. *PLoS One* 3(2):e1588.
14. Oh EC, et al. (2007) Transformation of cone precursors to functional rod photoreceptors by bZIP transcription factor NRL. *Proc Natl Acad Sci USA* 104(5):1679–1684.
15. Wu F, Sapkota D, Li R, Mu X (2012) Onecut 1 and Onecut 2 are potential regulators of mouse retinal development. *J Comp Neurol* 520(5):952–969.
16. Brzezinski JA, IV, Prasov L, Glaser T (2012) Math5 defines the ganglion cell competence state in a subpopulation of retinal progenitor cells exiting the cell cycle. *Dev Biol* 365(2):395–413.
17. Feng L, et al. (2010) MATH5 controls the acquisition of multiple retinal cell fates. *Mol Brain* 3:36.
18. Kay JN, Finger-Baier KC, Roeser T, Staub W, Baier H (2001) Retinal ganglion cell genesis requires lakritz, a Zebrafish atonal Homolog. *Neuron* 30(3):725–736.
19. Wang SW, et al. (2001) Requirement for math5 in the development of retinal ganglion cells. *Genes Dev* 15(1):24–29.
20. Brown NL, Patel S, Brzezinski J, Glaser T (2001) Math5 is required for retinal ganglion cell and optic nerve formation. *Development* 128(13):2497–2508.
21. Ghiasvand NM, et al. (2011) Deletion of a remote enhancer near ATOH7 disrupts retinal neurogenesis, causing NCRNA disease. *Nat Neurosci* 14(5):578–586.
22. Mu X, et al. (2004) Discrete gene sets depend on POU domain transcription factor Brn3b/Brn-3.2/POU4f2 for their expression in the mouse embryonic retina. *Development* 131(6):1197–1210.
23. Mu X, Fu X, Beremand PD, Thomas TL, Klein WH (2008) Gene regulation logic in retinal ganglion cell development: Isl1 defines a critical branch distinct from but overlapping with Pou4f2. *Proc Natl Acad Sci USA* 105(19):6942–6947.
24. Mu X, et al. (2005) A gene network downstream of transcription factor Math5 regulates retinal progenitor cell competence and ganglion cell fate. *Dev Biol* 280(2): 467–481.

25. Pan L, Deng M, Xie X, Gan L (2008) ISL1 and BRN3B co-regulate the differentiation of murine retinal ganglion cells. *Development* 135(11):1981–1990.
26. Gan L, et al. (1996) POU domain factor Brn-3b is required for the development of a large set of retinal ganglion cells. *Proc Natl Acad Sci USA* 93(9):3920–3925.
27. Xiang M (1998) Requirement for Brn-3b in early differentiation of postmitotic retinal ganglion cell precursors. *Dev Biol* 197(2):155–169.
28. Gan L, Wang SW, Huang Z, Klein WH (1999) POU domain factor Brn-3b is essential for retinal ganglion cell differentiation and survival but not for initial cell fate specification. *Dev Biol* 210(2):469–480.
29. Li R, et al. (2014) Isl1 and Pou4f2 form a complex to regulate target genes in developing retinal ganglion cells. *PLoS ONE* 9(3):e92105.
30. Liu W, et al. (2000) All Brn3 genes can promote retinal ganglion cell differentiation in the chick. *Development* 127(15):3237–3247.
31. Liu W, Mo Z, Xiang M (2001) The Ath5 proneural genes function upstream of Brn3 POU domain transcription factor genes to promote retinal ganglion cell development. *Proc Natl Acad Sci USA* 98(4):1649–1654.
32. Hutcheson DA, Vetter ML (2001) The bHLH factors Xath5 and XNeuroD can upregulate the expression of XBrn3d, a POU-homeodomain transcription factor. *Dev Biol* 232(2):327–338.
33. Qiu F, Jiang H, Xiang M (2008) A comprehensive negative regulatory program controlled by Brn3b to ensure ganglion cell specification from multipotential retinal precursors. *J Neurosci* 28(13):3392–3403.
34. Badea TC, Cahill H, Ecker J, Hattar S, Nathans J (2009) Distinct roles of transcription factors brn3a and brn3b in controlling the development, morphology, and function of retinal ganglion cells. *Neuron* 61(6):852–864.
35. Sprengel R, Hasan MT (2007) Tetracycline-controlled genetic switches. *Handb Exp Pharmacol* 178:49–72.
36. Livet J, et al. (2007) Transgenic strategies for combinatorial expression of fluorescent proteins in the nervous system. *Nature* 450(7166):56–62.
37. Szymczak AL, et al. (2004) Correction of multi-gene deficiency in vivo using a single 'self-cleaving' 2A peptide-based retroviral vector. *Nat Biotechnol* 22(5):589–594.
38. Brown NL, et al. (1998) Math5 encodes a murine basic helix-loop-helix transcription factor expressed during early stages of retinal neurogenesis. *Development* 125(23): 4821–4833.
39. Le TT, Wroblewski E, Patel S, Riesenberg AN, Brown NL (2006) Math5 is required for both early retinal neuron differentiation and cell cycle progression. *Dev Biol* 295(2): 764–778.
40. Pacal M, Bremner R (2014) Induction of the ganglion cell differentiation program in human retinal progenitors before cell cycle exit. *Dev Dyn* 243(5):712–729.
41. Prasov L, Glaser T (2012) Dynamic expression of ganglion cell markers in retinal progenitors during the terminal cell cycle. *Mol Cell Neurosci* 50(2):160–168.
42. Gao Z, Mao CA, Pan P, Mu X, Klein WH (2014) Transcriptome of Atoh7 retinal progenitor cells identifies new Atoh7-dependent regulatory genes for retinal ganglion cell formation. *Dev Neurobiol* 74(11):1123–1140.
43. Jiang Y, et al. (2013) Transcription factors SOX4 and SOX11 function redundantly to regulate the development of mouse retinal ganglion cells. *J Biol Chem* 288(25): 18429–18438.
44. Wang Y, Dakubo GD, Thurig S, Mazerolle CJ, Wallace VA (2005) Retinal ganglion cell-derived sonic hedgehog locally controls proliferation and the timing of RGC development in the embryonic mouse retina. *Development* 132(22):5103–5113.
45. Mu X, et al. (2005) Ganglion cells are required for normal progenitor- cell proliferation but not cell-fate determination or patterning in the developing mouse retina. *Curr Biol* 15(6):525–530.
46. Sanes JR, Zipursky SL (2010) Design principles of insect and vertebrate visual systems. *Neuron* 66(1):15–36.
47. Sweeney NT, Tierney H, Feldheim DA (2014) Tbr2 is required to generate a neural circuit mediating the pupillary light reflex. *J Neurosci* 34(16):5447–5453.
48. Mao CA, et al. (2008) Eomesodermin, a target gene of Pou4f2, is required for retinal ganglion cell and optic nerve development in the mouse. *Development* 135(2): 271–280.
49. Mao CA, et al. (2014) T-box transcription regulator Tbr2 is essential for the formation and maintenance of Opn4/melanopsin-expressing intrinsically photosensitive retinal ganglion cells. *J Neurosci* 34(39):13083–13095.
50. Kay JN, et al. (2011) Retinal ganglion cells with distinct directional preferences differ in molecular identity, structure, and central projections. *J Neurosci* 31(21):7753–7762.
51. Haverkamp S, Wässle H (2000) Immunocytochemical analysis of the mouse retina. *J Comp Neurol* 424(1):1–23.
52. Sagdullaev BT, Eggers ED, Purgert R, Lukasiewicz PD (2011) Nonlinear interactions between excitatory and inhibitory retinal synapses control visual output. *J Neurosci* 31(42):15102–15112.
53. Sethuramanujam S, Slaughter MM (2014) Disinhibitory recruitment of NMDA receptor pathways in retina. *J Neurophysiol* 112(1):193–203.
54. Taschenberger H, Engert F, Grantyn R (1995) Synaptic current kinetics in a solely AMPA-receptor-operated glutamatergic synapse formed by rat retinal ganglion neurons. *J Neurophysiol* 74(3):1123–1136.
55. Chen X, Hsueh HA, Greenberg K, Werblin FS (2010) Three forms of spatial temporal feedforward inhibition are common to different ganglion cell types in rabbit retina. *J Neurophysiol* 103(5):2618–2632.
56. Freed MA, Smith RG, Sterling P (2003) Timing of quantal release from the retinal bipolar terminal is regulated by a feedback circuit. *Neuron* 38(1):89–101.
57. Xu PX, Woo I, Her H, Beier DR, Maas RL (1997) Mouse Eya homologues of the Drosophila eyes absent gene require Pax6 for expression in lens and nasal placode. *Development* 124(1):219–231.
58. Prasov L, Nagy M, Rudolph DD, Glaser T (2012) Math5 (Atoh7) gene dosage limits retinal ganglion cell genesis. *Neuroreport* 23(10):631–634.
59. Nickells RW (2012) The cell and molecular biology of glaucoma: Mechanisms of retinal ganglion cell death. *Invest Ophthalmol Vis Sci* 53(5):2476–2481.
60. Nickells RW, Howell GR, Soto I, John SW (2012) Under pressure: Cellular and molecular responses during glaucoma, a common neurodegeneration with axonopathy. *Annu Rev Neurosci* 35:153–179.
61. Sluch VM, Zack DJ (2014) Stem cells, retinal ganglion cells and glaucoma. *Dev Ophthalmol* 53:111–121.
62. Al-Shamekh S, Goldberg JL (2014) Retinal repair with induced pluripotent stem cells. *Transl Res* 163(4):377–386.
63. Karl MO (2013) The potential of stem cell research for the treatment of neuronal damage in glaucoma. *Cell Tissue Res* 353(2):311–325.
64. George SH, et al. (2007) Developmental and adult phenotyping directly from mutant embryonic stem cells. *Proc Natl Acad Sci USA* 104(11):4455–4460.
65. Office of Laboratory Animal Welfare (2002) *Public Health Service Policy on Human Care and Use of Laboratory Animals.* Available at grants.nih.gov/grants/olaw/references/phspol.htm. Accessed March 5, 2015.
66. Sapkota D, et al. (2014) Onecut1 and Onecut2 redundantly regulate early retinal cell fates during development. *Proc Natl Acad Sci USA* 111(39):E4086–E4095.
67. Wu F, et al. (2013) Onecut1 is essential for horizontal cell genesis and retinal integrity. *J Neurosci* 33(32):13053–13065.

Supporting Information

Wu et al. 10.1073/pnas.1421535112

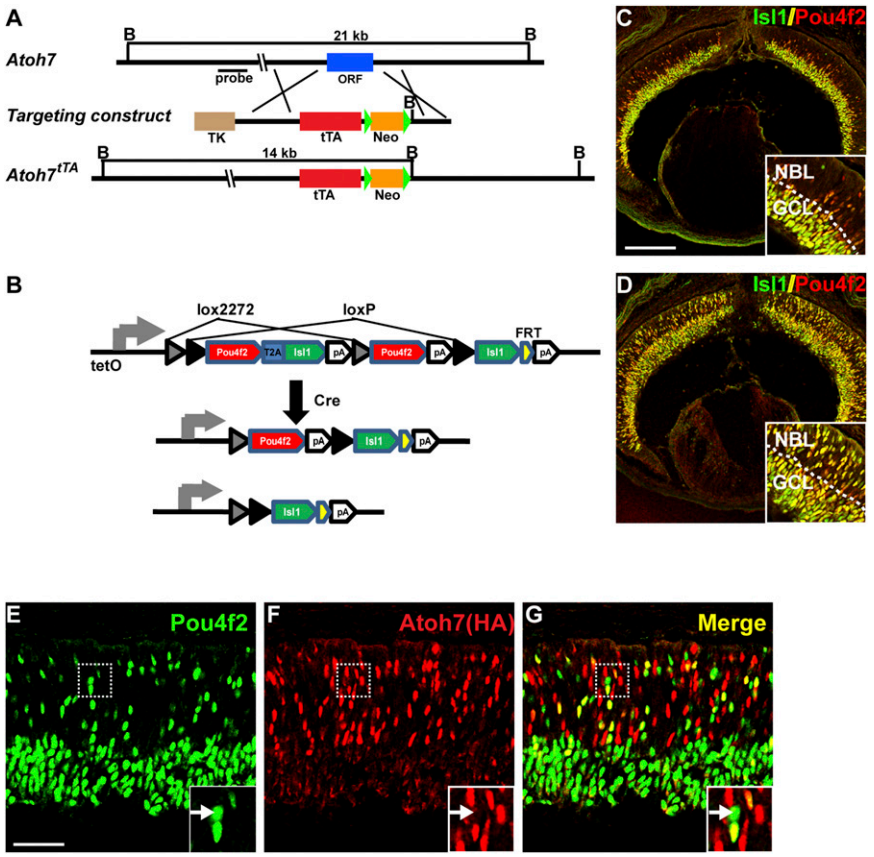

Fig. S1. Strategy for expressing Isl1 and Pou4f2 in Atoh7-expressing cells in the absence of Atoh7. (*A*) Generation of the *Atoh7*^{tTA} knockin allele by homologous recombination. Structures of the wild-type *Atoh7* allele, targeting construct, and targeted allele *Atoh7*^{tTA} are shown. Green triangles are loxP sites, and TK indicates the thymidine kinase cassette used for negative selection. (*B*) Generation of the *tetO-P&I* transgenic allele. The construct design and the generation of two other alleles by Cre-mediated recombination are shown. (*C*) Immunofluorescence staining of E14.5 *Atoh7*$^{tTA/+}$ retinal sections for Pou4f2 and Isl1, marking both newly emerging RGCs in the NBL and those that already have migrated to the GCL. (Scale bar, 150 μm.) (*D*) Immunostaining of Pou4f2 and Isl1 on *Atoh7* $^{tTA/+}$*;tetO-P&I* retinal sections. There are more cells expressing Pou4f2 and Isl1 in the NBL than in the *Atoh7*$^{tTA/+}$ control, indicating that the *tetO-P&I* transgene is activated by tTA from the *Atoh7*^{tTA} allele. (*E–G*) Coimmunostaining of Pou4f2 and Atoh7 (HA) on E14.5 *Atoh7* $^{tTA/HA}$*;tetO-P&I* retinal sections. Most Pou4f2^{+} cells in the NBL are also Atoh7(HA)$^{+}$, but some cells have little or very low Atoh7(HA) (arrow in *Insets*), indicating the *Atoh7* promoter has been turned off. In contrast, many Atoh7(HA)$^{+}$ cells do not express Pou4f2, implying a delay from the activation of the *Atoh7* promoter to the expression of Pou4f2. (Scale bar, 37.5 μm.)

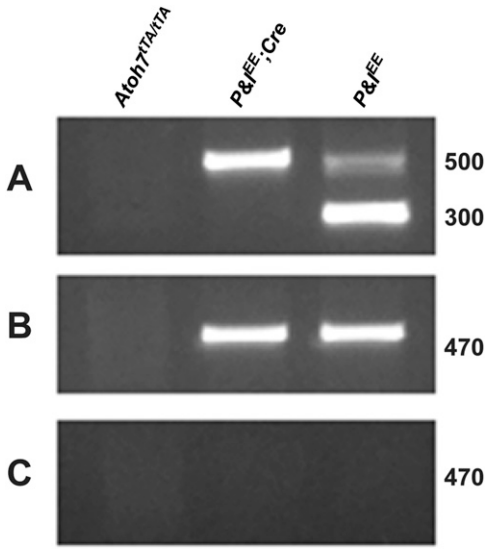

Fig. S2. Examination of Cre-induced recombination of the *tetO-P&I* transgene in the *P&I*^{EE}*;Cre* retina by PCR. See Fig. S1*A* for the structure of the transgene and possible outcomes after Cre recombination. Genomic DNA from retinas of the indicated genotypes was analyzed by three PCR reactions. Reaction A detects both the *Pou4f2-T2A-Isl1* cassette (300 bp) and the other two cassettes when present (500 bp). The absence of the 300-bp band in the *P&I*^{EE}*;Cre* mouse indicates that the *Pou4f2-T2A-Isl1* cassette is efficiently deleted by Cre, as expected. Reaction B detects either the *Pou4f2-T2A-Isl1* cassette or the *Pou4f2* cassette when brought next to the *tetO* promoter by Cre. The sizes (~470 bp) are very close and could not be resolved on the gel. Because the *Pou4f2-T2A-Isl1* is absent in the *P&I*^{EE}*;Cre* mice, the detection of the 470-bp band indicates that the *Pou4f2* cassette is brought next to the *tetO* promoter. Reaction C detects the *Isl1* cassette only when it is next to the *tetO* promoter after recombination. We did not detect the expected band (470 bp), suggesting the designed recombination did not occur, but the reason is unknown. These results are consistent with the immunostaining data shown in Fig. 1 *C*–*C*′′. Primers used in reaction A are forward: 5′-CGA AAA GCT GGA TCT CAA GA-3′ and reverse: 5′-AAT ACT GAT TAC ACT CCG CA-3′. Primers in reaction B are forward: 5′-TAT CAG TGA ATG AGA AAA GTG-3′ and reverse: 5′-ACT GTG TAG CGC CGA GTA CTT-3′. Primers in reaction C are forward: 5′-TAT CAG TGA ATG AGA AAA GTG-3′ and reverse: 5′-AAT ACT GAT TAC ACT CCG CAC-3′.

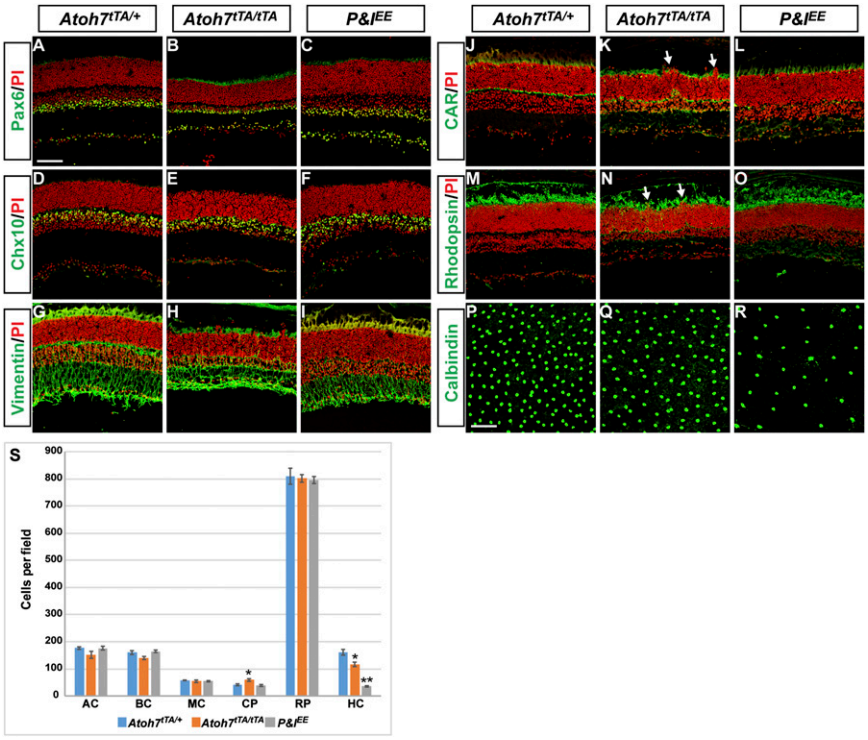

Fig. S3. Other cell types in the *P&I*^{EE} retina. (*A–O*) Immunofluorescence staining of retinal sections from P30 retinas with the different genotypes (as indicated) using antibodies to various cell-type–specific markers (green): Pax6 for amacrine cells (*A–C*); Chx10 for bipolar cells (*D–F*); Vimentin for Müller glial cells (*G–I*); cone arrestin (CAR) for cone photoreceptors (*J–L*); and rhodopsin for rod photoreceptors (*M–O*). Nuclei are stained with propidium iodide (red). Arrows in *K* and *N* point to areas of disrupted lamination in the *Atoh7*-null retina. (Scale bar, 75 μm.) (*P–R*) Flat-mount immunostaining for calbindin to label horizontal cells in the *Atoh7*$^{tTA/+}$ (*P*), *Atoh7*$^{tTA/tTA}$ (*Q*), and *P&I*^{EE} (*R*) retinas at P30. (Scale bar, 75 μm.) (*S*) Counting of the various cell types in retinas with the different genotypes. AC, amacrine cells; BC, bipolar cells; CP, cone photoreceptors; HC, horizontal cells; MC, Müller cells; RP, rod photoreceptors. *$P < 0.1$, **$P < 0.01$ in comparison with *Atoh7*$^{tTA/+}$, as determined by Student's *t* test. Error bars indicate ± SD.